

Nuclear Cross Sections Analysis and R-matrix Tools - Minischool  
Surrey Ion Beam Centre and Department of Physics  
University of Surrey, Thursday May 9th – Friday May 10th 2013

*Leverhulme Lecture III*  
**Similarities between Nuclear Data  
for IBA and Astrophysics**

Alexander Gurbich



Leverhulme Professor

*Surrey University Ion Beam Centre*



*On leave from the Institute for Physics and Power  
Engineering, Obninsk, Russia*

# Goals of Nuclear Astrophysics

- To understand what is the energy source of the stars at all stages of their evolution
- To explain the observed relative abundances of the elements through the nuclear transmutations in different stellar conditions

## Aims of IBA

- To determine composition and structure of thin films or surface layers of samples through the spectroscopy of the products of the interaction of accelerated charged particles with nuclei contained in the sample.

# Similarities

- Low energy charged particle cross-sections play a key role.
- Calculated (evaluated) cross-sections rather than measured ones are commonly used.
- The same physical models are employed in the calculations.

# Distinctions

## Nuclear Astrophysics

## IBA

Cross-sections are needed for a vast variety of stable and unstable nuclei	Cross-sections for a limited number of mainly light and medium weight nuclei are of interest
Cross-sections are needed for separate isotopes	Cross-sections are needed mostly averaged over isotopes
Total cross-sections are needed	Differential cross-sections are needed
Moderate requirements for the precision	The required precision is ~1%.
The problem is explored by nuclear physicists	The problem is being solved by IBA (material science) community
Basic (fundamental) science	Applied (technological) science

# Alpha-process in stars

A so called alpha-process is responsible for the synthesis of alpha cluster nuclei in the chain:



It takes place in stars during carbon and oxygen burning at temperature in the interval of  $(0.5\text{--}3.0) \times 10^9 \text{ K}$  (43–260 keV).

# Alpha elastic scattering in IBA

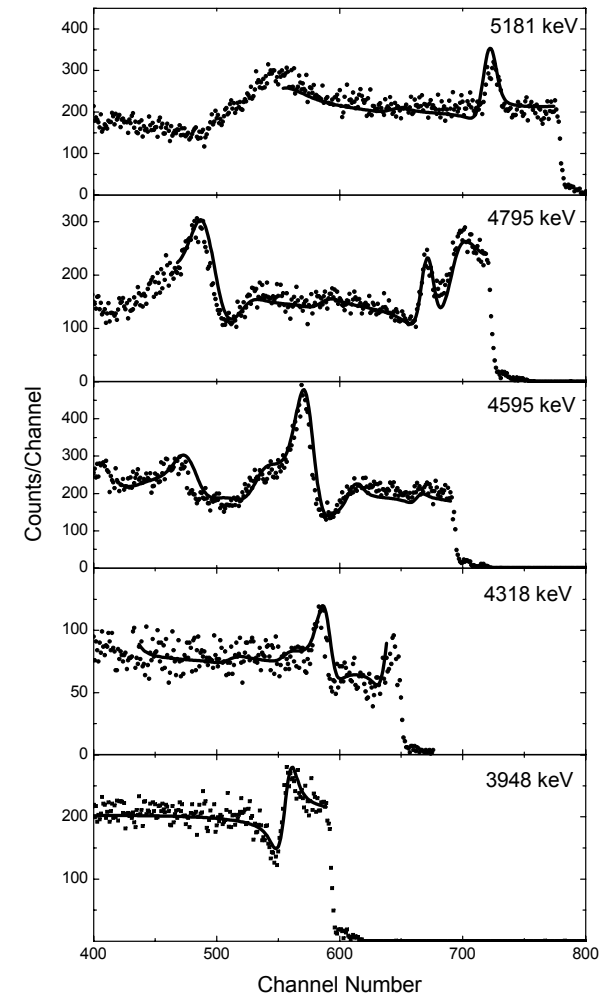
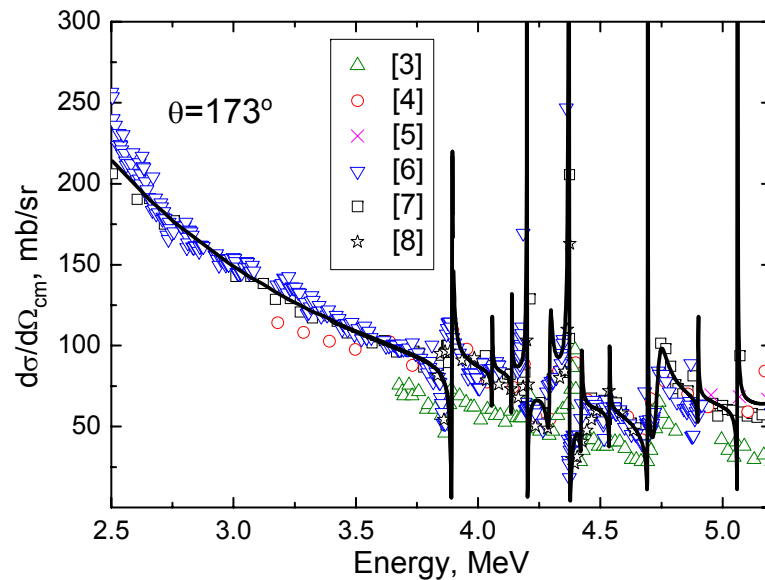
There are a number of benefits in use of elastic backscattering (EBS) technique at energies for which the cross-section is non-Rutherford.

First of all at higher energies light ion elastic scattering cross section for light elements rapidly increases whereas it still follows close to  $1/E^2$  energy dependence for heavy nuclei. Thus high sensitivity for determination of light contaminants in heavy matrix is achieved. Besides, a depth of sample examination is enhanced.

# Alpha elastic scattering in IBA

Spectra of alphas  
backscattered from a thick  
silicon sample

Evaluated  $^{28}\text{Si}(\alpha, \alpha)^{28}\text{Si}$  cross-section



# Cross-section calculations for alpha-process

The cross section for this process is usually calculated by means of the *statistical model*. The *transmission coefficients* which are central quantities in such calculations are determined in frameworks of the *optical model*. It is usual in nuclear astrophysics to consider processes that incorporate a wide variety of nuclei both stable and unstable and so the main efforts so far were concentrated on the development of a global optical potential using microscopic approach.



# Microscopic global optical potential



Nuclear Physics A 707 (2002) 253–276



[www.elsevier.com/locate/npe](http://www.elsevier.com/locate/npe)

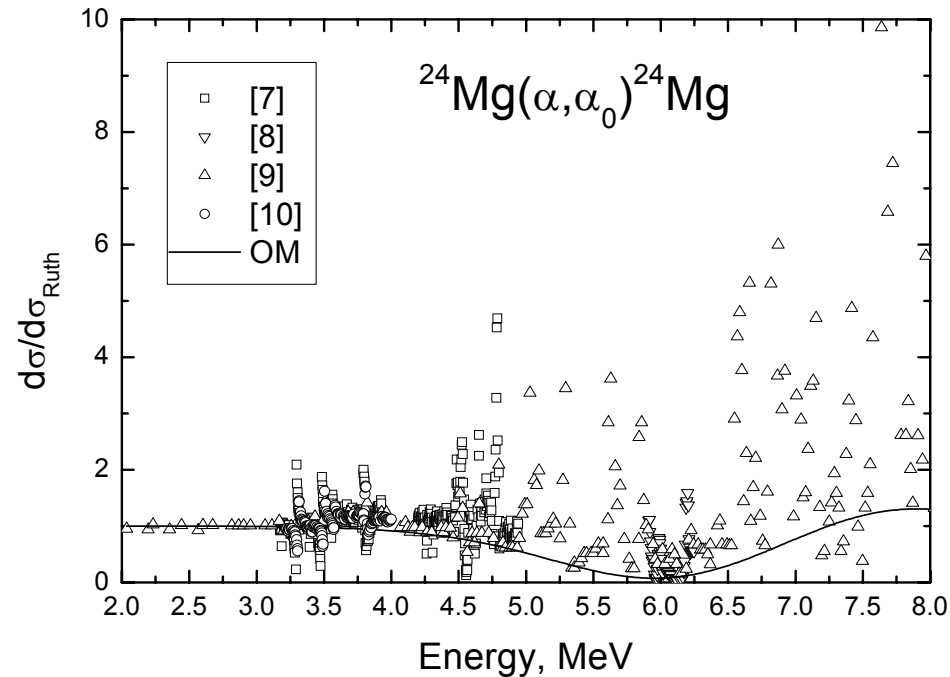
## Improved global $\alpha$ -optical model potentials at low energies

P. Demetriou<sup>a,\*</sup>, C. Grama<sup>b</sup>, S. Goriely<sup>c</sup>

---

The nuclei under consideration are stable and a lot of experimental information is available in the literature for the interaction of alphas with these nuclei. Consequently a phenomenological optical potential can be obtained in this case.

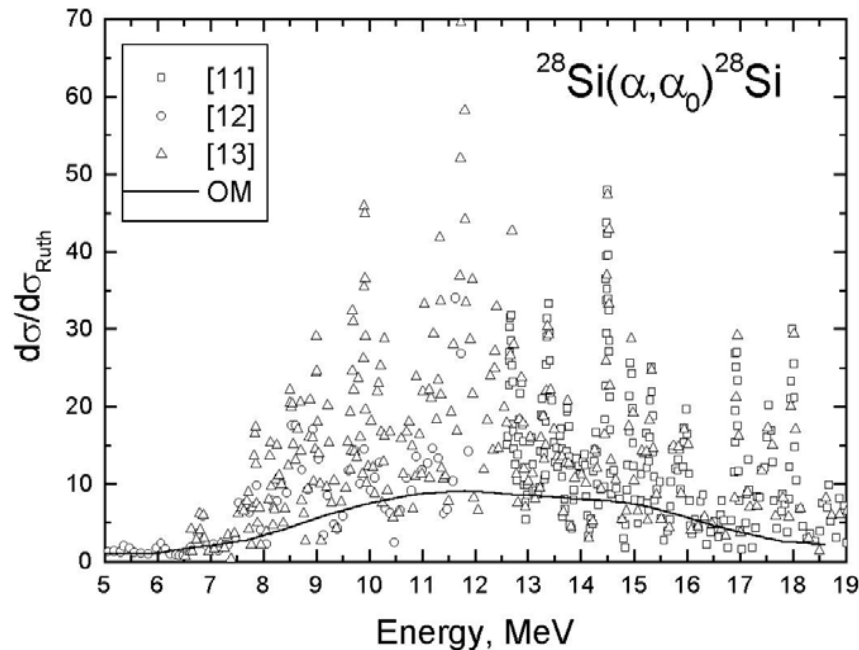
# Alpha optical potential for $^{24}\text{Mg}$



Available experimental data and results of the optical model calculations for  $^{24}\text{Mg}(\alpha, \alpha_0)^{24}\text{Mg}$  at the scattering angle close to  $165^\circ$ .

The optimal potential parameters obtained for $^{24}\text{Mg}(\alpha, \alpha_0)^{24}\text{Mg}$ scattering at the energy below 8.0 MeV									
$V_{l=0}$ MeV	$V_{l=1}$ MeV	$V_{l=2}$ MeV	$V_{l=3}$ MeV	$V_{l=4}$ MeV	$V_{l \geq 5}$ MeV	$W_D$ MeV	$r$ fm	$a$ fm	$r_c$ fm
225	235	215	215	215	225	9.0	1.40	0.52	1.40

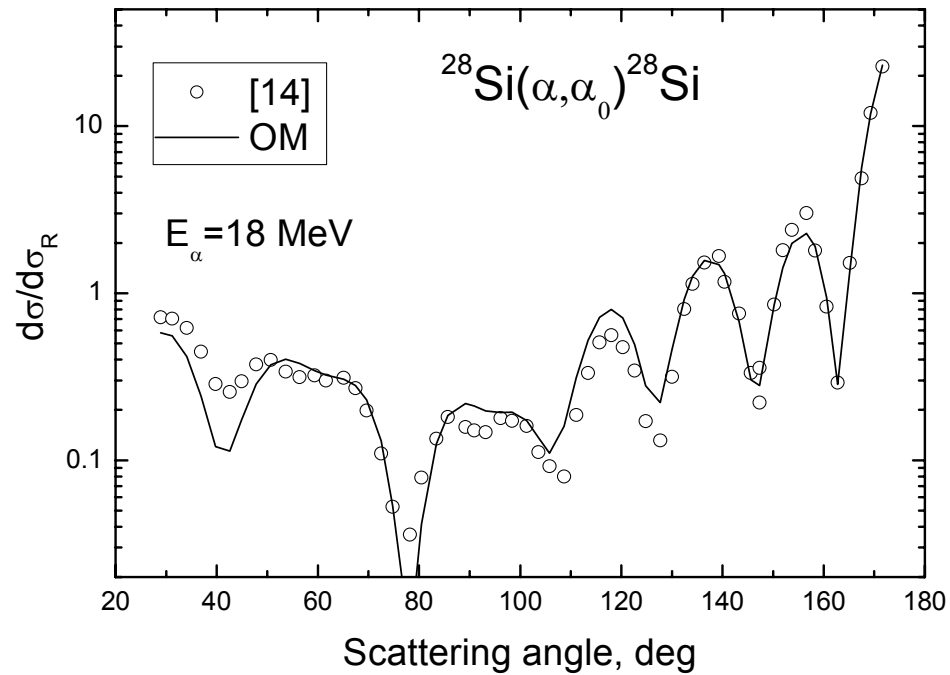
# Alpha optical potential for $^{28}\text{Si}$



Available experimental data and results of the optical model calculations for  $^{28}\text{Si}(\alpha, \alpha_0)^{28}\text{Si}$  excitation function at the scattering angle close to  $170^\circ$ .

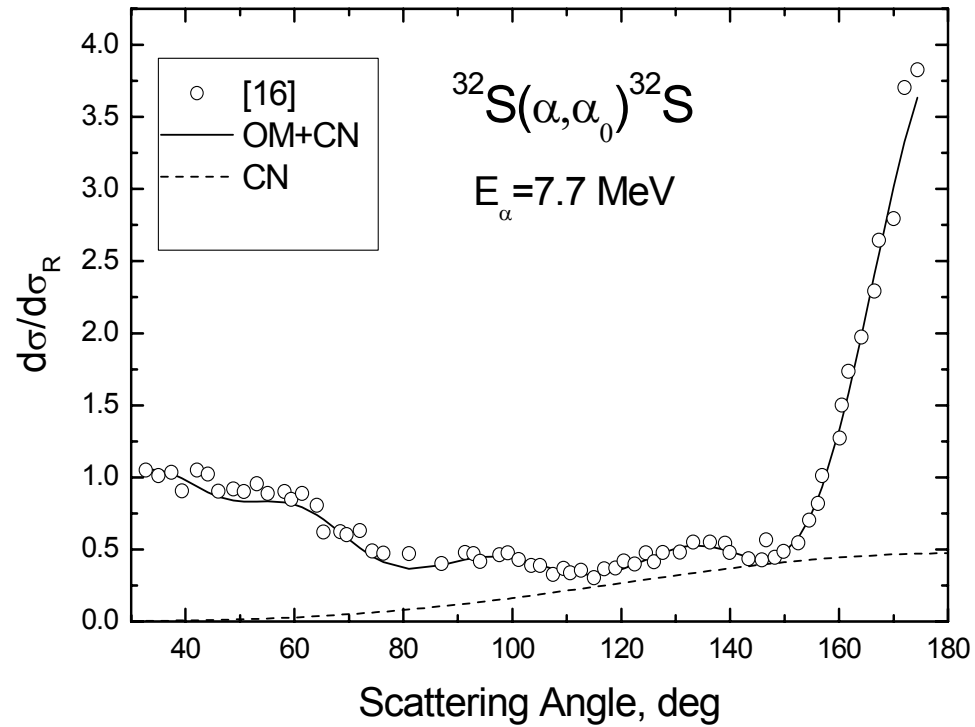
The optimal potential parameters obtained for $^{28}\text{Si}(\alpha, \alpha_0)^{28}\text{Si}$ scattering at low energy											
$V_{l=0}$ MeV	$V_{l=1}$ MeV	$V_{l=2}$ MeV	$V_{l=3}$ MeV	$V_{l=4}$ MeV	$V_{l \geq 5}$ MeV	$W_D$ MeV	$r_R$ fm	$a_R$ fm	$r_D$ fm	$a_D$ fm	$r_C$ fm
155.7	159.0	157.9	156.5	155.1	156.8	$1.79+0.57E$	1.40	0.914	1.40	0.62	1.40

# Alpha optical potential for $^{28}\text{Si}$



The best fit to the angular distribution for  $^{28}\text{Si}(\alpha, \alpha_0)^{28}\text{Si}$  at 18 MeV.

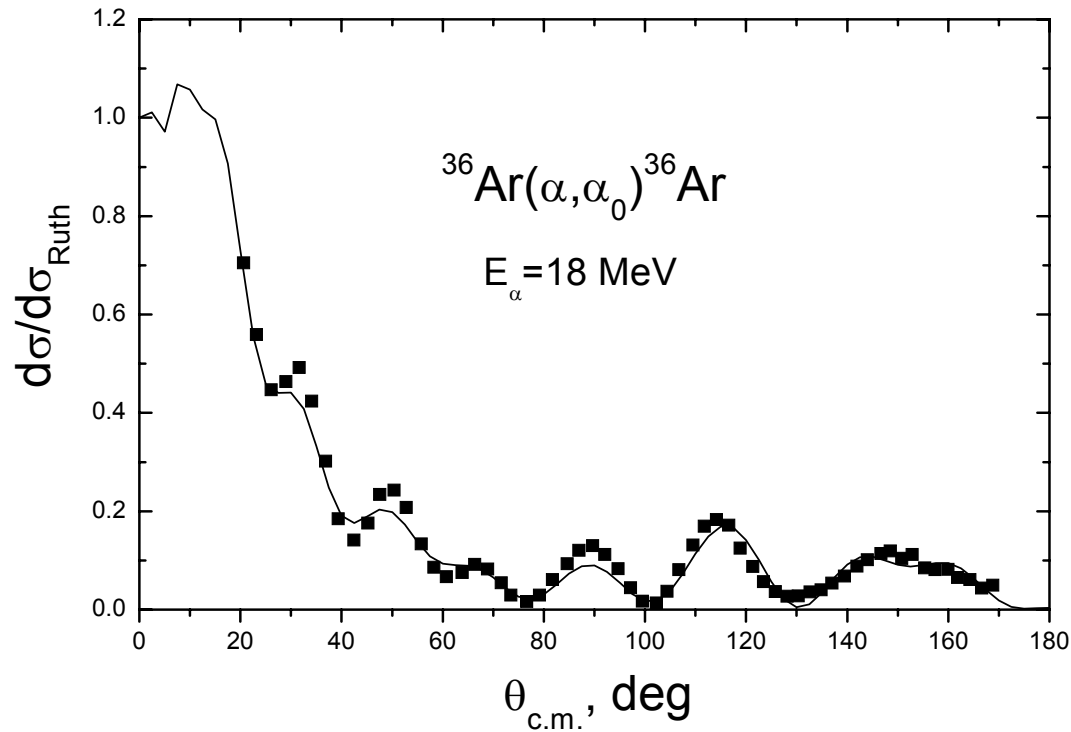
# Alpha optical potential for $^{32}\text{S}$



The best fit to the angular distribution for  $^{32}\text{S}(\alpha, \alpha_0)^{32}\text{S}$  at 7.7 MeV.

The optimal potential parameters obtained for $^{32}\text{S}(\alpha, \alpha_0)^{32}\text{S}$ scattering at the energy of 7.7 MeV											
$V_{l=0}$ MeV	$V_{l=1}$ MeV	$V_{l=2}$ MeV	$V_{l=3}$ MeV	$V_{l=4}$ MeV	$V_{l \geq 5}$ MeV	$W_D^*$ MeV	$r_R^*$ fm	$a_R$ fm	$r_D$ fm	$a_D^*$ fm	$r_C^*$ fm
125.9	139.9	148.6	136.1	132.3	133.5	7.0	1.4	0.77	1.4	0.485	1.40

# Alpha optical potential for $^{36}\text{Ar}$

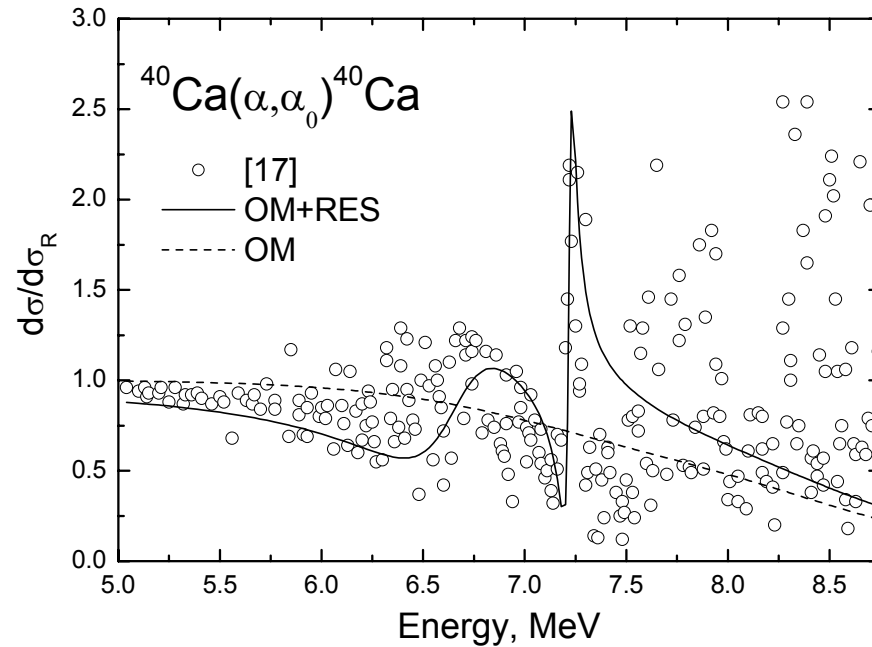


The best fit to the angular distribution for  $^{36}\text{Ar}(\alpha, \alpha_0)^{36}\text{Ar}$  at 18 MeV.

The optimal potential parameters obtained for  $^{36}\text{Ar}(\alpha, \alpha_0)^{36}\text{Ar}$  scattering at the energy of 18 MeV

$V_{l=0}$ MeV	$V_{l=1}$ MeV	$V_{l=2}$ MeV	$V_{l=3}$ MeV	$V_{l=4}$ MeV	$V_{l \geq 5}$ MeV	$W_D^*$ MeV	$r_R^*$ fm	$a_R$ fm	$r_D$ fm	$a_D^*$ fm	$r_C^*$ fm
135.6	125.4	131.0	141.9	145.5	143.7	14.0	1.281	0.749	1.625	0.485	1.30

# Alpha optical potential for $^{40}\text{Ar}$



The effect of quasimolecular resonances on the excitation function for  $^{40}\text{Ca}(\alpha, \alpha_0)^{40}\text{Ca}$  at the scattering angle of  $167^\circ$ .

$$S_l = \exp(2i\lambda_l) \left[ \exp(-2\mu_l) + \exp(2i\phi) \frac{i\Gamma_\alpha}{E_0 - E - \frac{1}{2}i\Gamma} \right]$$

# Statistical model

The statistical model predicts reaction cross sections averaged over many resonances in the intermediate nuclei. The mean angle-integrated cross section for formation of the final state ( $E'$ ,  $I'$ ,  $P'$ ) by means of the ( $a, a'$ ) reaction is given as

$$\sigma_{a,a'}(\epsilon, I, P; E', I', P') = \sum_{J, \pi} \sigma_a(\epsilon, I, P; U, J, \pi) \frac{\Gamma_{a'}(U, J, \pi; E', I', P')}{\Gamma(U, J, \pi)} , \quad (2)$$

where  $(U, J, \pi)$  are the quantum numbers of the compound states through which the reactions proceed;  $\sigma_a(\epsilon, I, P; U, J, \pi)$  is the reaction cross section for formation of the compound nucleus with quantum numbers  $(U, J, \pi)$ ; and  $\Gamma_{a'}(U, J, \pi; E', I', P')$  is the decay width of the compound nucleus into the state  $(E', I', P')$  of the residual nucleus by emission of the particle  $a'$ . The quantity  $\Gamma(U, J, \pi)$  is the total decay width of the compound nucleus state  $(U, J, \pi)$  and is the sum of all possible decay widths,

$$\Gamma(U, J, \pi) = \sum_{a''} \sum_{E'', I'', P''} \Gamma_{a''}(U, J, \pi; E'', I'', P'') , \quad (3)$$



# Transmission coefficients

The reaction cross section for formation of the compound nucleus can be expressed in terms of optical model transmission coefficients,  $T_\ell^a(\epsilon)$ , as follows:

$$\sigma_a(\epsilon, I, P; U, J, \pi) = \frac{\pi}{k^2} \frac{(2J+1)}{(2I+1)(2i+1)} \sum_{S=|I-i|}^{I+i} \sum_{\ell=|J-S|}^{J+S} f_\ell(\ell, \pi) T_\ell^a(\epsilon), \quad (4)$$

where  $k$  is the wave number of relative motion,  $S$  indicates channel spin, and the function  $f(\ell, \pi)$  is unity if parity is conserved and zero otherwise, as provided by Eq. (1). Through use of the reciprocity theorem (detailed balance) of nuclear reactions, the decay widths can be related to the transmission coefficients:

$$\Gamma_a(U, J, \pi; E', I', P') = \frac{1}{2\pi\rho(U, J, \pi)} \sum_{S=|I'-I'|}^{I'+I'} \sum_{\ell=|J-S|}^{J+S} f(\ell, \pi) T_\ell^{a'}(U-E'-B_{a'}) \quad (5)$$

where  $\rho(U, J, \pi)$  is the nuclear level density of the intermediate nucleus having the quantum numbers  $(U, J, \pi)$ . To obtain Eq. (5), the assumption is made that the optical model transmission coefficients, determined from analysis of experimental data on the ground states of nuclei, also describe the inverse reactions on excited states of the residual nuclei.

# Statistical model calculations with global potential

Atomic Data and Nuclear Data Tables **75**, 1–351 (2000)

doi:10.1006/adnd.2000.0834, available online at <http://www.idealibrary.com> on **IDEAL**<sup>®</sup>

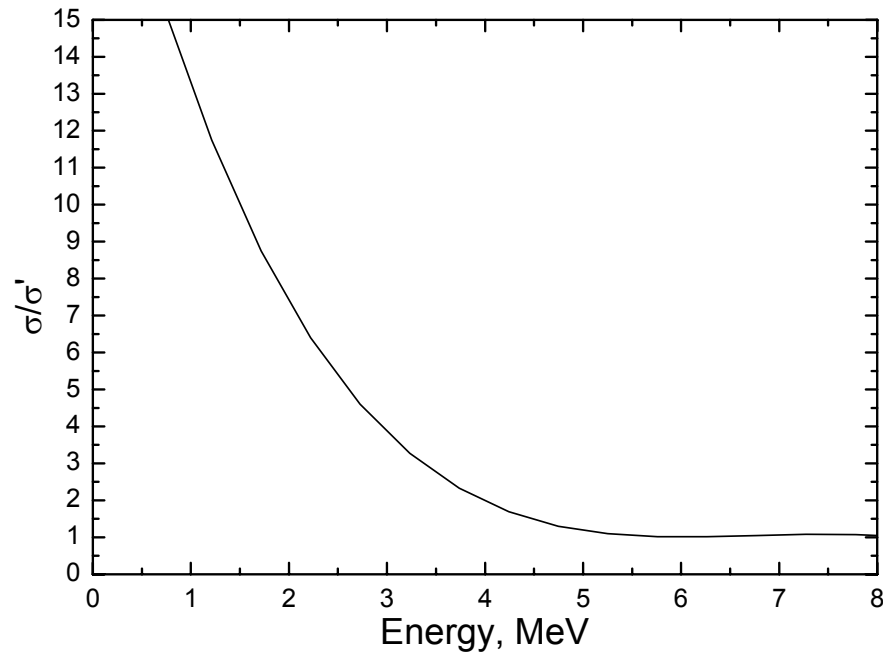


## ASTROPHYSICAL REACTION RATES FROM STATISTICAL MODEL CALCULATIONS

THOMAS RAUSCHER and FRIEDRICH-KARL THIELEMANN

Departement für Physik und Astronomie, Universität Basel, Klingelbergstrasse 82  
CH-4056 Basel, Switzerland

# Comparison of statistical calculations with transmission coefficients obtained using different optical potentials



The ratio of the cross sections for the  $^{28}\text{Si}(\alpha, \gamma)^{32}\text{S}$  reaction calculated with transmission coefficients obtained with the optical potential of the present work and with the global potential.

# Elastic scattering of alphas from carbon

## IBA

The fact that the  $^{12}\text{C}(\alpha, \alpha)^{12}\text{C}$  cross-section is up to 100 times larger than Rutherford above 2 MeV is used for analytical purposes. The intense resonance at 4.26 MeV is used as a powerful tool for carbon profiling in various substrates.

## Nuclear Astrophysics

An improvement in the elastic scattering data helps to determine the contribution of the subthreshold states, 6.92(2<sup>+</sup>) and 7.12(1<sup>-</sup>) MeV and restricts resonance parameters above the threshold.

## Carbon analysis using energetic ion beams

W. Jiang <sup>\*</sup>, V. Shutthanandan, S. Thevuthasan, D.E. McCready, W.J. Weber

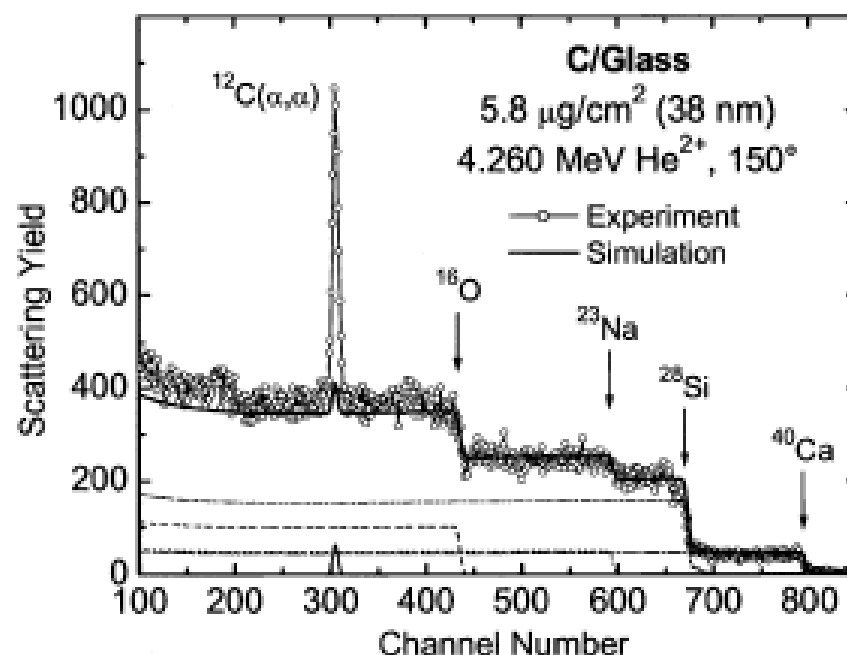
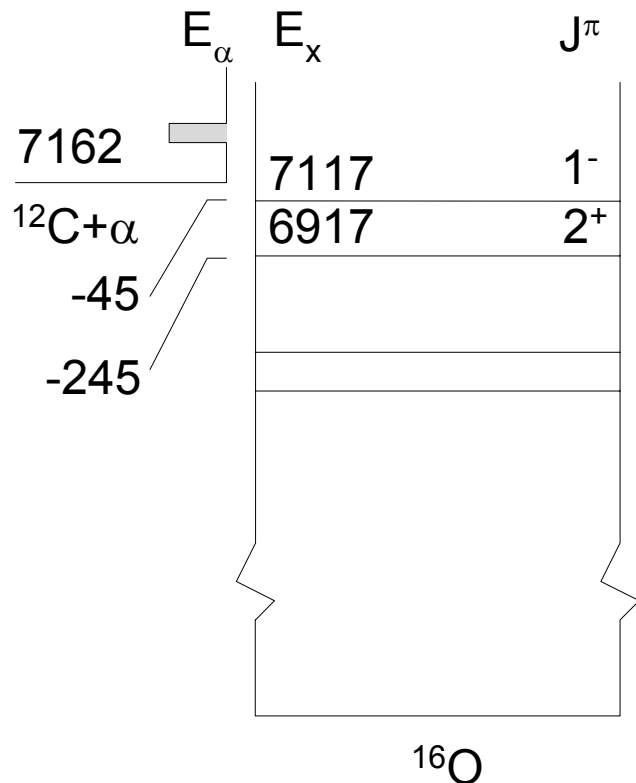


Fig. 2. Energy spectrum of 4.260 MeV  $\text{He}^{2+}$  backscattering from a thin carbon film (5.8  $\mu\text{g}/\text{cm}^2$ ) on a silicate glass substrate at an angle of 150°. Also included are the elemental and entire spectra from SIMNRA simulations.

# The problem of $^{12}\text{C}/^{16}\text{O}$ ratio in nucleosynthesis



The ratio depends on the rate of the  $3\alpha \rightarrow ^{12}\text{C}$  and  $^{12}\text{C}(\alpha, \gamma)^{16}\text{O}$  reactions.

The cross-section for  $3\alpha \rightarrow ^{12}\text{C}$  is known with accuracy  $\sim 15\%$

For the  $^{12}\text{C}(\alpha, \gamma)^{16}\text{O}$  reaction extrapolation is made from  $\sim 1.4$  MeV (the lowest energy at which the measurements were performed) to  $\sim 0.3$  MeV, the cross-section decreasing from  $\sim 10^{-10}$  to  $10^{-17}$  barn.

The main contribution to the cross-section at astrophysical energies comes from E1 and E2 amplitudes produced by subthreshold levels.

# Measurement of elastic $^{12}\text{C} + \alpha$ scattering: Details of the experiment, analysis, and discussion of phase shifts

P. Tischhauser,<sup>\*</sup> A. Couture,<sup>†</sup> R. Detwiler,<sup>‡</sup> J. Görres, C. Ugalde,<sup>§</sup> E. Stech, and M. Wiescher

*University of Notre Dame, Department of Physics, Notre Dame, Indiana 46556, USA*

M. Heil<sup>||</sup> and F. Käppeler

*Forschungszentrum Karlsruhe, Institut für Kernphysik, Postfach 3640, D-76021 Karlsruhe, Germany*

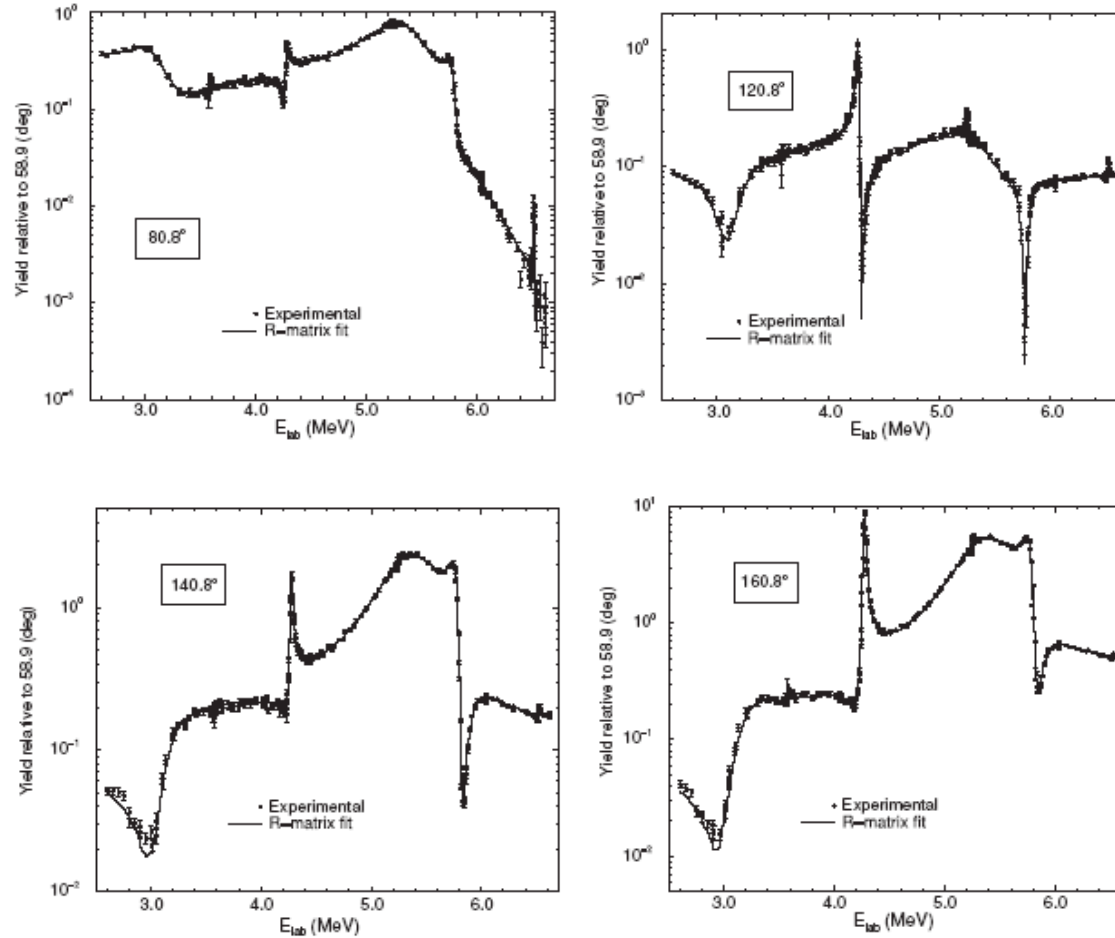


FIG. 6. Relative differential cross-section excitation curves for  $^{12}\text{C}(\alpha, \alpha)^{12}\text{C}$  for eight selected detector angles  $\theta = 24^\circ, 38^\circ, 54^\circ, 79^\circ, 100^\circ, 120^\circ, 140^\circ$ , and  $160^\circ$ .

# Measurement of elastic $^{12}\text{C} + \alpha$ scattering: Above the proton separation energy

R. J. deBoer,<sup>\*</sup> A. Couture,<sup>†</sup> R. Detwiler,<sup>‡</sup> J. Görres, P. Tischhauser,<sup>§</sup> E. Überseder, C. Ugalde,<sup>||</sup> E. Stech, and M. Wiescher  
*Department of Physics, University of Notre Dame, Notre Dame, Indiana 46556, USA*

R. E. Azuma  
*Department of Physics, University of Notre Dame, Notre Dame, Indiana 46556, USA, and*  
*Department of Physics, University of Toronto, Toronto, Ontario M5S 1A7, Canada*

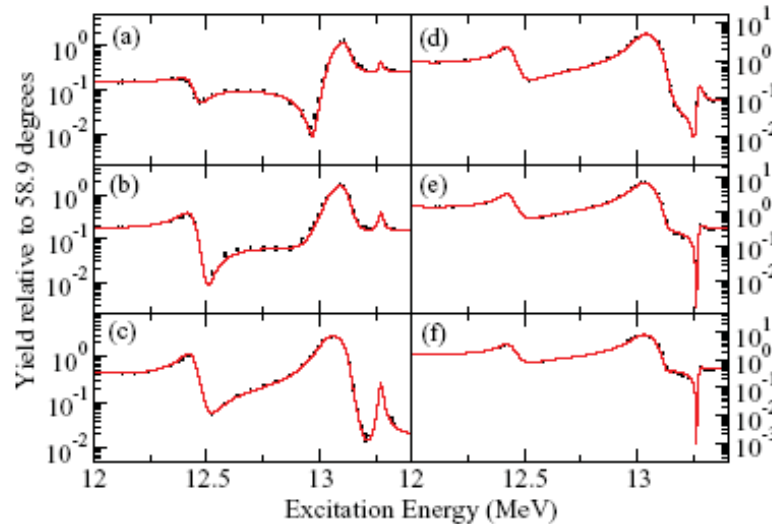


FIG. 6. (Color online) Fits to the  $^{12}\text{C}(\alpha, \alpha_0)^{12}\text{C}$  yield data of this work at  $\theta_{\text{lab}} = 125.8^\circ$  (a),  $130.8^\circ$  (b),  $140.8^\circ$  (c),  $150.8^\circ$  (d),  $160.8^\circ$  (e), and  $165.9^\circ$  (f). The  $R$ -matrix fit was performed simultaneously with previous data from the literature.

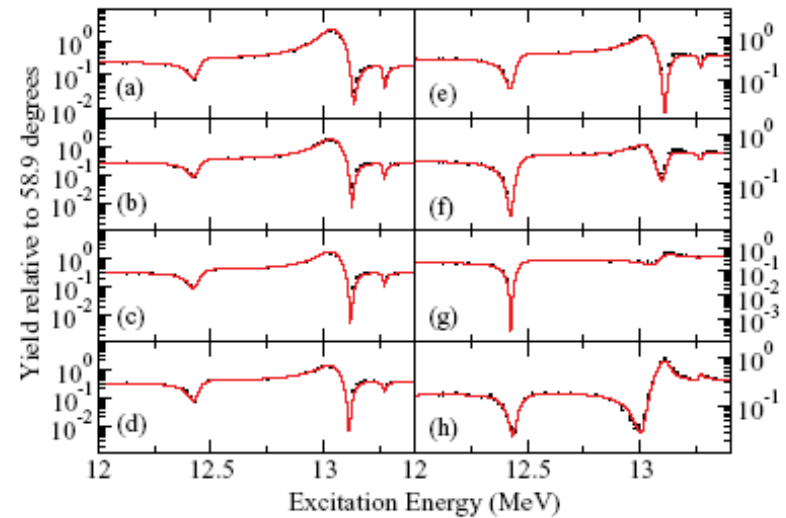


FIG. 5. (Color online) Fits to the  $^{12}\text{C}(\alpha, \alpha_0)^{12}\text{C}$  yield data of this work at  $\theta_{\text{lab}} = 95.8^\circ$  (a),  $99.0^\circ$  (b),  $100.8^\circ$  (c),  $103.9^\circ$  (d),  $105.8^\circ$  (e),  $110.8^\circ$  (f),  $115.8^\circ$  (g), and  $120.8^\circ$  (h). The  $R$ -matrix fit was performed simultaneously with previous data from the literature.



# Evaluation of the cross-section for elastic scattering of $^4\text{He}$ from carbon

A.F. Gurbich \*

*Institute of Physics and Power Engineering, Bondarenko Square 1, 249020 Obninsk, Russian Federation*

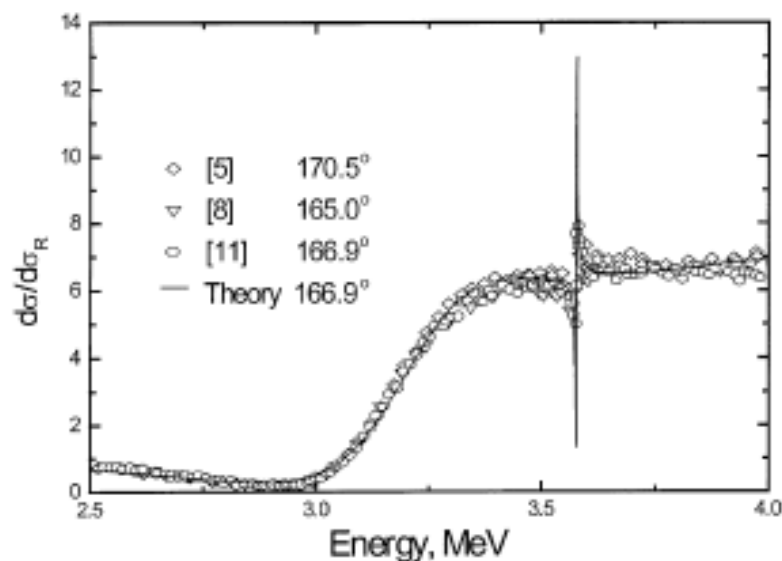


Fig. 1. The available experimental data and the evaluated excitation function for  $^4\text{He}$  elastic scattering from carbon in the energy range from 2.5 to 4.0 MeV.

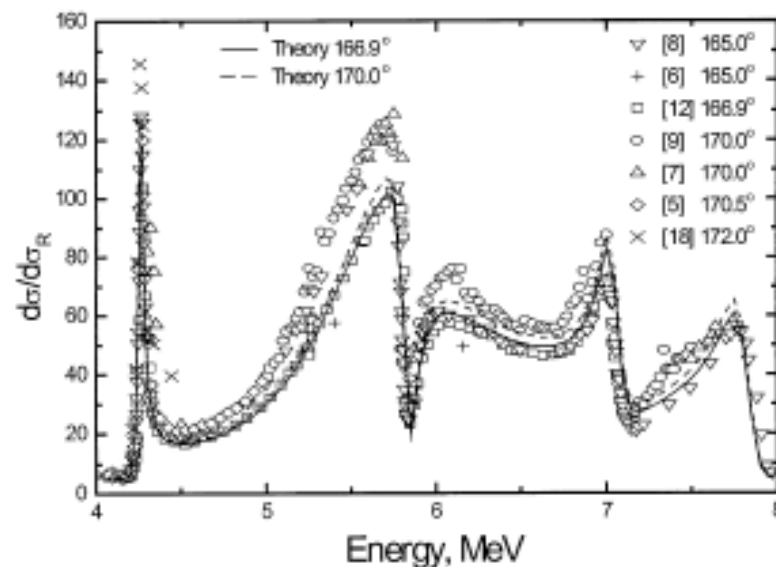


Fig. 2. The same as in Fig. 1, in the energy range from 4.0 to 8.0 MeV.

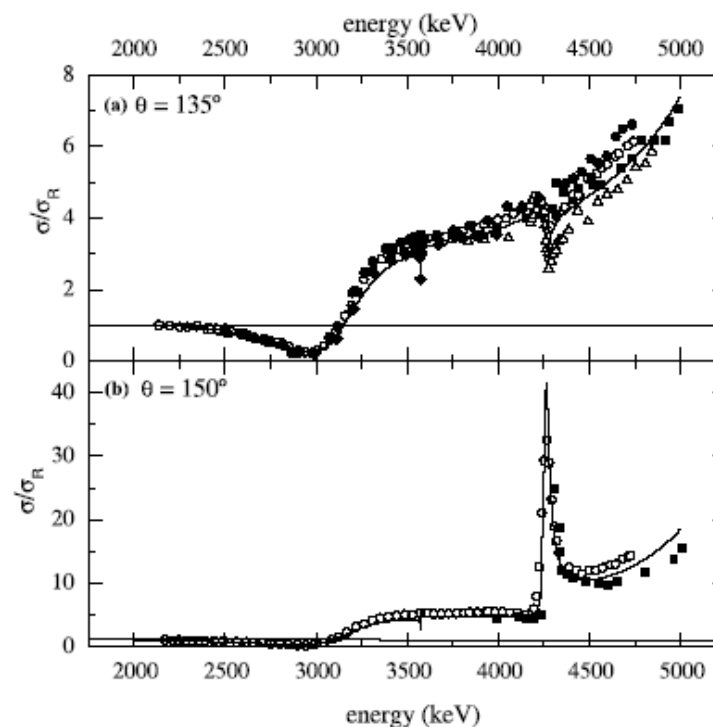
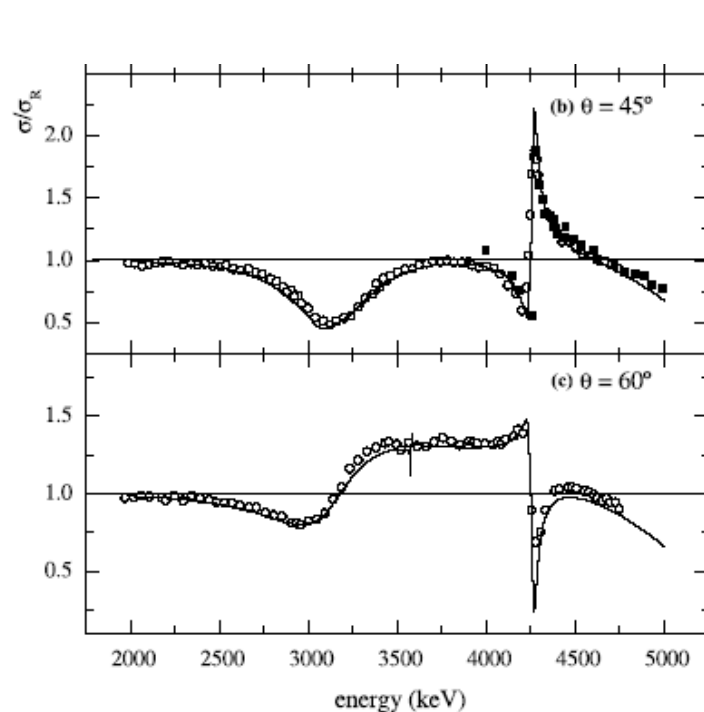
# Helium elastic scattering from carbon for 30° to 150° in the energy region from 2 to 4.8 MeV

I. Bogdanović Radović <sup>a,\*</sup>, M. Jakšić <sup>a</sup>, O. Benka <sup>b</sup>, A.F. Gurbich <sup>c</sup>

<sup>a</sup> Ruder Bošković Institute, P.O. Box 1016, 10000 Zagreb, Croatia

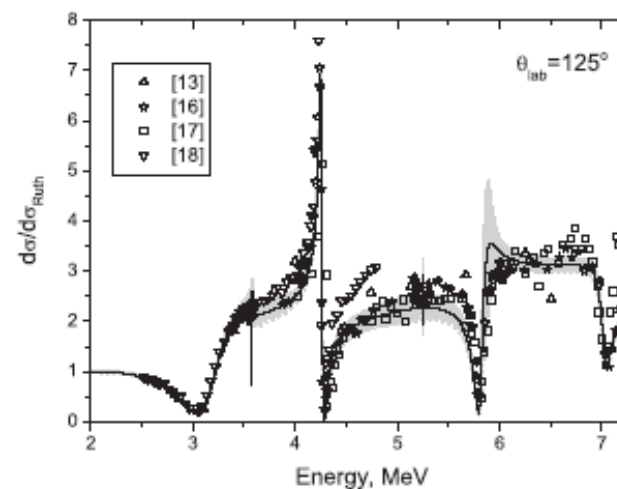
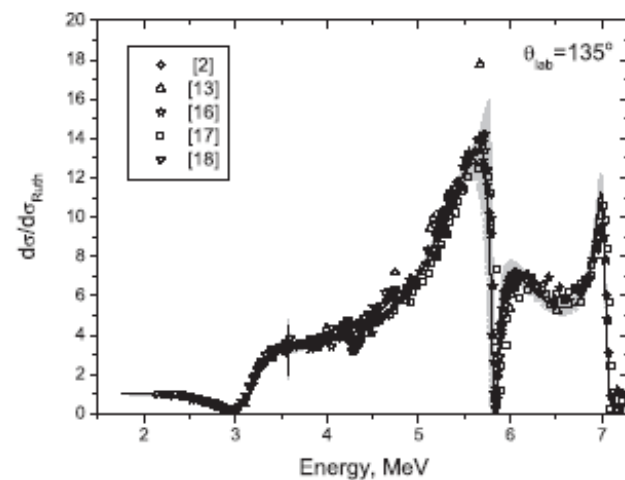
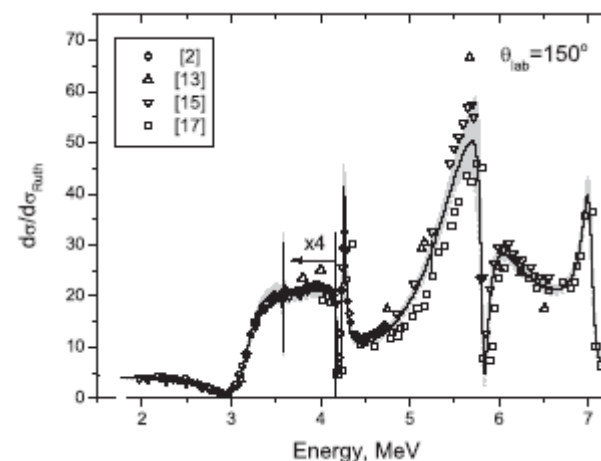
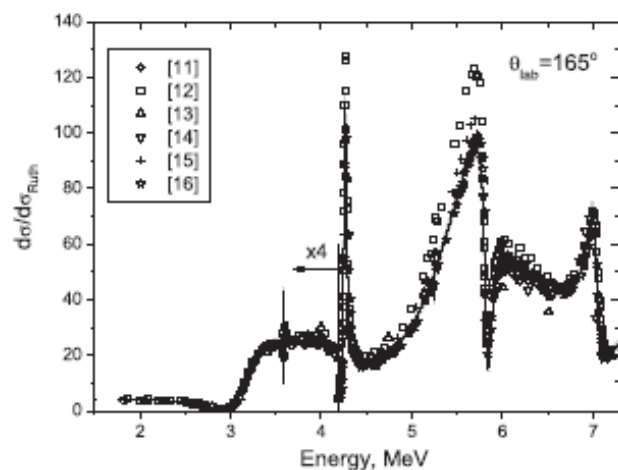
<sup>b</sup> Institut für Experimentalphysik, Johannes Kepler-Universität Linz, 4040 Linz, Austria

<sup>c</sup> Institute of Physics and Power Engineering, 249020 Obninsk, Russia



Evaluated  $^{12}\text{C}(^4\text{He}, ^4\text{He})^{12}\text{C}$  cross-section and its uncertainty

E.V. Gai, A.F. Gurbich\*

*Institute for Physics and Power Engineering, Bondarenko sq. 1, 249033 Obninsk, Russian Federation*

# CRP on PIGE



**IAEA**

International Atomic Energy Agency

INDC(NDS)-0625

Distr. IBA

## **INDC International Nuclear Data Committee**

Summary Report

2<sup>nd</sup> Research Coordination Meeting

**Development of a Reference Database for  
Particle-Induced Gamma ray Emission (PIGE)  
Spectroscopy**

# Cross-section measurements for PIGE

## 4. Action lists

Table 4.1. Completed Measurements

Isotope	Reaction	$\gamma$ -ray [keV]	Energy range [MeV]	Angle [°]	Initial State, $J^\pi$	Type of Data	Comments	Measured by:
$^7\text{Li}$	$(p,p'\gamma)$	478	2-4	130	1/2-	Differential+Thick target	Detailed+sparse points	Pedro de Jesus
$^9\text{Be}$	$(p,\gamma)$	718	0.5-1.7	130	1+	Differential+Thick target	Detailed	Pedro de Jesus
$^{10}\text{B}$	$(p,\alpha'\gamma)$	429	2-4	130	1/2-	Thick target	Sparse points	Pedro de Jesus
$^{12}\text{C}$	$(p,\gamma)$		1.1-2.6	55 and 0		Differential	Detailed	Becker
$^{14}\text{N}$	$(p,p'\gamma)$	2313	4-7	55	0+	Differential	Detailed+sparse points	Raisanen
$^{14}\text{N}$	$(d,p'\gamma)$	1885	0.6-2	55	5/2+	Differential	Detailed+sparse points	Kiss
$^{14}\text{N}$	$(d,p'\gamma)$	2297	0.6-2	55	7/2+	Differential	Detailed+sparse points	Kiss
$^{14}\text{N}$	$(d,p'\gamma)$	8310	0.6-2	55	1/2+	Differential	Detailed+sparse points	Kiss
$^{19}\text{F}$	$(p,p'\gamma)$	110	2-4	130	1/2-	Differential+Thick target	Detailed	Pedro de Jesus
$^{19}\text{F}$	$(p,p'\gamma)$	197	2-4	130	5/2+	Differential+Thick target	Detailed	Pedro de Jesus
$^{19}\text{F}$	$(p,\alpha'\gamma)$	6000-7000	0.8-4.0	130	3-	Differential+Thick target	Detailed	Pedro de Jesus

# $^{16}\text{O}(\alpha,\gamma)^{20}\text{Ne}$ $S$ factor: Measurements and $R$ -matrix analysis

H. Costantini,<sup>1,2</sup> R. J. deBoer,<sup>2,\*</sup> R. E. Azuma,<sup>2,3</sup> M. Couder,<sup>2</sup> J. Görres,<sup>2</sup> J. W. Hammer,<sup>2,†</sup> P. J. LeBlanc,<sup>2</sup> H. Y. Lee,<sup>4</sup>  
 S. O'Brien,<sup>2</sup> A. Palumbo,<sup>2</sup> E. C. Simpson,<sup>5</sup> E. Stech,<sup>2</sup> W. Tan,<sup>2</sup> E. Uberseder,<sup>2</sup> and M. Wiescher<sup>2</sup>

<sup>1</sup>*Istituto Nazionale di Fisica Nucleare, Sezione di Genova, Genova, Italy*

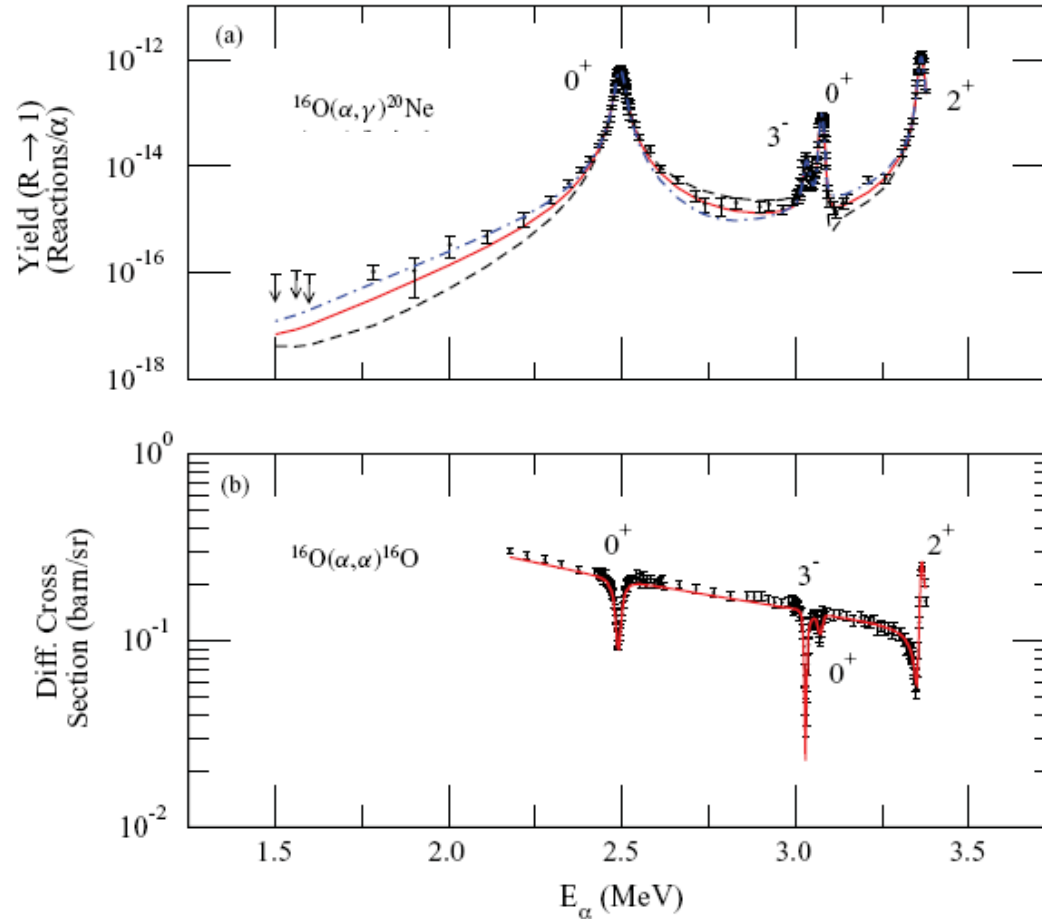
<sup>2</sup>*Department of Physics, University of Notre Dame, Notre Dame, Indiana 46556, USA*

<sup>3</sup>*Department of Physics, University of Toronto, Toronto, Ontario M5S 1A7, Canada*

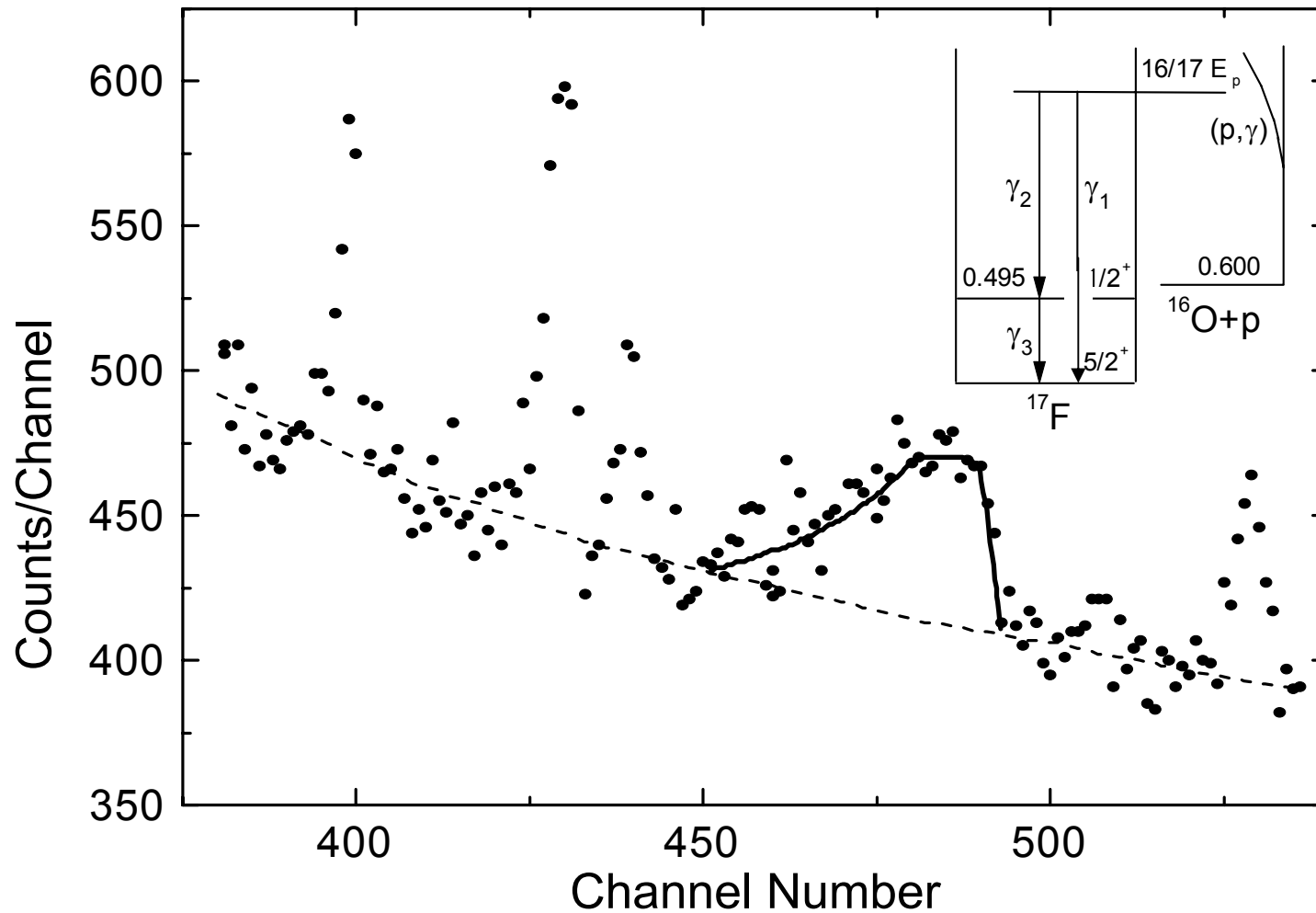
<sup>4</sup>*LANLSC-NE, Los Alamos National Laboratory, New Mexico 87545, USA*

<sup>5</sup>*Department of Physics, Faculty of Engineering and Physical Sciences, University of Surrey, Guildford, Surrey GU2 7XH, United Kingdom*

(Received 28 June 2010; published 13 September 2010)



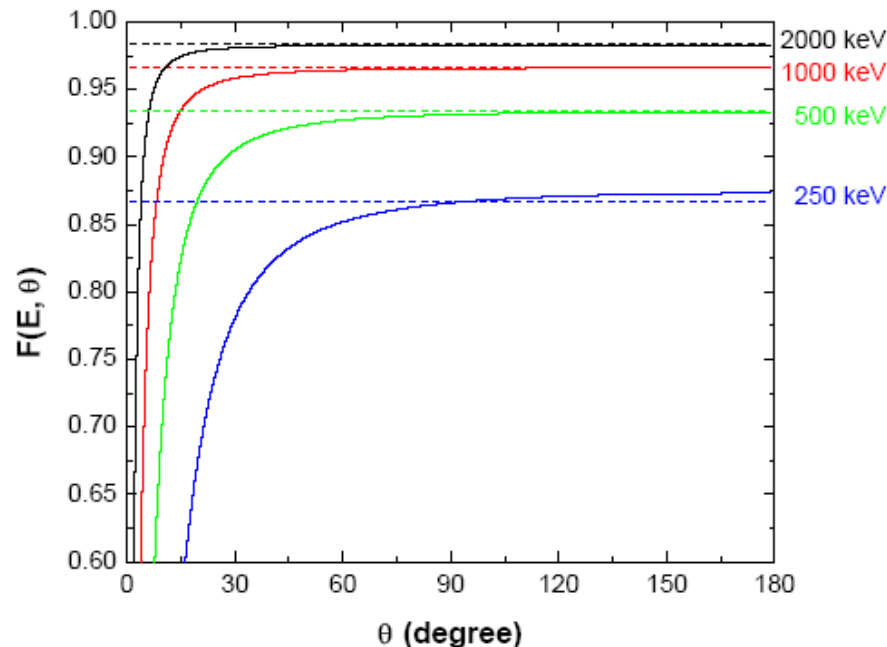
# Oxygen analysis using gammas from direct non-resonant radiative capture



$$E_{\gamma}(E_p) = \frac{M}{M+m} E_p(x) + Q - E_1 - \Delta E_{\gamma} \quad \sigma(E_p) \varepsilon(E_{\gamma}(E_p)) \approx \text{const}$$

$$N(E_{\gamma}, \theta) \delta E = \frac{N_A}{M} q \Omega c(x) \varepsilon(E_{\gamma}(E_p(x))) \sigma(E_p(x), \theta) \frac{\delta x}{\cos \varphi}$$

# Electron screening effects in IBA



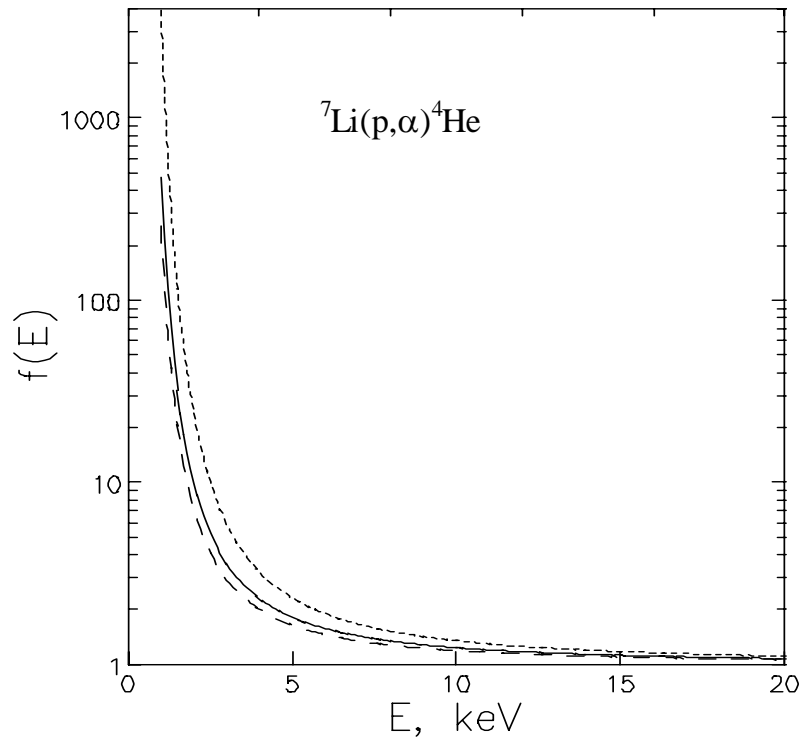
Correction factors for Rutherford cross-section – L'Ecuyer (dashed lines and Andersen (solid line) at different energies

$$F_{\text{L'Ecuyer}} = 1 - \frac{0.049 Z_1 Z_2^{4/3}}{E_{CM}} \quad F_{\text{Andersen}} = \frac{\left(1 + \frac{1}{2} \frac{V_1}{E_{CM}}\right)^2}{\left\{1 + \frac{V_1}{E_{CM}} + \left[\frac{V_1}{2E_{CM} \sin \theta_{CM}/2}\right]^2\right\}^2}$$

$$\sigma = F \sigma_R$$



# Electron screening effects in nuclear astrophysics



The cross-sections measured in a laboratory should be corrected to the stellar conditions where nuclei are bare.

$$f(E) = \frac{\sigma_{\text{exp}}(E)}{\sigma_{BN}(E)},$$

# CONCLUSIONS



## **INDC International Nuclear Data Committee**

### **Summary Report of the Technical Meeting on Long-term Needs for Nuclear Data Development**

IAEA Headquarters, Vienna, Austria

2 – 4 November 2011

There is a significant overlap between astrophysics and other nuclear physics applications. Important experimental and theoretical efforts are made by the astrophysics community that can be of interest and of direct relevance to nuclear applications and vice-versa the progress made in the various applications can be of direct relevance for nuclear astrophysics. On this basis, it is recommended to the IAEA:

to continuously identify overlap of interest between astrophysics and other nuclear applications and possible cross-fertilization between the various communities...